Nanocrystals

DOI: 10.1002/anie.200604167

High-Yield Synthesis of Single-Crystalline Gold Nano-octahedra**

*Cuncheng Li, Kevin L. Shuford, Q.-Han Park, Weiping Cai, Yue Li, Eun Je Lee, and Sung Oh Cho**

Metal nanostructures have been the focus of intensive research because of their unique chemical and physical properties.[1] Among them, nanostructured Au and Ag have attracted considerable attention mainly as a result of their remarkable optical properties and numerous applications, such as surface plasmonics, surface-enhanced Raman scattering (SERS), chemical and biological sensing, and photothermal therapy.[1–3] The intrinsic properties of a metal nanostructure strongly depend on its size and shape. The synthesis of metal nanostructures with tailored size and shape is thus important for uncovering their size- and shape-dependent properties and for realizing their practical applications. In the last few years, a variety of synthetic strategies for metal nanostructures have been developed in aqueous or nonhydrolytic media, the strategies include photochemistry,[4] thermochemistry,[5] wet-chemistry,[6] and biochemistry.[7] Using these strategies, a myriad of shape-controlled Au and Ag nanostructures, such as wires,[5a,8] rods,[6b,8b,9] sheets,[5,10] prisms,[4,7,11] belts,[12] and branched multipods,[6b,13] have been routinely synthesized in high yield. In addition, some polyhedral Au and Ag nanocrystals (cubes,[6b,7a,14–16] tetrahedra,[16a] octahedra,[17] decahedra,[17a] icosahedra,[16a] and bipyramids[18]) have also been prepared in large quantities in recent years. However, selective synthesis of uniform, octahedral Au nanocrystals in high yield, with well-defined shape and tunable size has not been accomplished. Herein, we present a modified polyol process to mass-synthesize uniform, single-crystalline Au nanocrystals with octahedral shape, in which all eight faces are equilateral triangles and four triangles meet at each corner. The optical properties of the octahedral Au nanocrystals were firstly analyzed with the theoretical calculation using the discrete-dipole approximation (DDA).[19]

The polyol process[20] is a convenient, versatile, and low-cost method for the synthesis of metal nanostructures on a large scale. Current polyol synthesis is mainly based on the use of ethylene glycol which acts both as a solvent of the precursors and as a reducing reagent for the reaction. A number of anisotropic metal nanostructures have been successfully synthesized in ethylene glycol solution on the basis of this technique.[5d,8,14,16,21] We recently found that octahedral Au particles of hundreds of nanometers in size were easily synthesized by replacing ethylene glycol with polyethylene glycol 600 (PEG 600). However, these Au octahedra were always mixed with many other kinds of Au nanostructures. It was difficult to study and utilize their properties because the yield of octahedral Au particles in the final product was lower than 15%.

Herein, a modified polyol process based on PEG 600 was developed to selectively synthesize octahedral Au nanocrystals in high yield. In this process, a small amount of sodium borohydride ($NaBH_4$) was added to a PEG 600 solution of polyvinylpyrrolidone (PVP) prior to the addition of a gold(III) chloride ($AuCl_3$) aqueous solution. The solution was then preheated at 75 °C for more than 24 h, then further heated at 125 °C for different reaction times from 6 h to 48 h. The products were collected by centrifugation and washed repeatedly with ethanol before characterization and study.

Field-emission scanning electron microscopy (FESEM) images show that the majority (> 90%) of the as-prepared product was octahedral nanoparticles (Figure 1 A,B). The mean edge length of the octahedral nanoparticles was 50 nm with a standard deviation of 5 nm. All the surfaces of the octahedral nanoparticles were smooth with no obvious defects (Figure 1 C). Energy dispersive X-ray spectrum (EDS) analysis confirms that the products consisted only of Au. The X-ray diffraction (XRD) pattern identified the nanoparticles as pure crystalline face-centered cubic (fcc) Au (Figure 1 D). The intensity ratio of the (200) and (111) diffraction peaks in the XRD pattern was 0.31, which is lower than the bulk value of 0.53. This result suggests that the Au nano-octahedra were abundant in {111} planes and, thus,

[*] Dr. C. Li, E. J. Lee, Prof. S. O. Cho
Department of Nuclear and Quantum Engineering
Korea Advanced Institute of Science and Technology
Daejeon 305-701 (Korea)
Fax: (+82) 42-869-3810
E-mail: socho@kaist.ac.kr
Dr. K. L. Shuford
Chemical Sciences Division
Oak Ridge National Laboratory
P.O. Box 2008 MS6142, Oak Ridge, TN 37-831 (USA)
Prof. Q.-H. Park
Department of Physics
Korea University
Seoul 136-701 (Korea)
Dr. C. Li, Prof. W. Cai, Dr. Y. Li
Institute of Solid State Physics
Chinese Academia of Sciences
Hefei 230-031, Anhui (P.R. China)
Dr. C. Li
Physical Science and Technology College
Zhengzhou University
Zhengzhou 450052, Henan (P.R. China)

[**] This work was supported by the Korea Science and Engineering Foundation (KOSEF) grant funded by the Korean government (MOST). K.L.S. was supported by the Wigner Fellowship and partially sponsored by the U.S. Department of Energy under contract DE-AC05-00OR22725 with Oak Ridge National Laboratory, managed and operated by UT-Battelle, LLC.

Supporting information for this article is available on the WWW under http://www.angewandte.org or from the author.

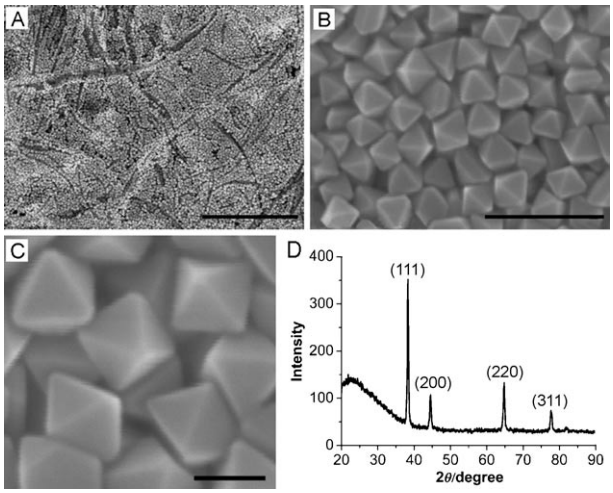

Figure 1. A) Low-magnification and B,C) high-magnification FESEM images of the Au nano-octahedra. D) X-ray diffraction pattern. Scale bars for (A), (B), and (C) are 2 μm, 200 nm, and 50 nm, respectively.

that their {111} planes tended to be preferentially oriented parallel to the surface of the supporting substrate.

A typical transmission electron microscopy (TEM) image of the Au nano-octahedra and the selected area electron diffraction (SAED) pattern are presented in Figure 2. The

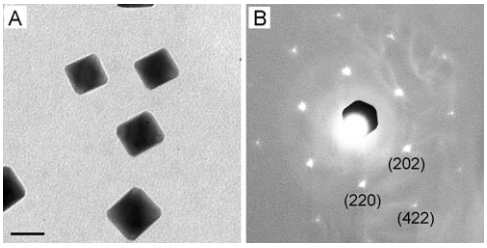

Figure 2. A) A typical TEM image of the Au nano-octahedra. B) The SAED pattern. The electron beam was perpendicular to one of the triangle faces of an individual octahedral particle. Scale bar for (A) is 50 nm.

SAED pattern was recorded by focusing the electron beam on one of the triangle faces of an Au nano-octahedron. The inner set of spots with the hexagonal symmetry was indexed to {220} reflections, which further revealed that each Au nano-octahedron was a single crystal with {111} lattice planes as the basal surfaces.

A series of color changes were observed during the modified polyol process. The color of the precursor solution changed from yellow to colorless after being preheated at 75 °C for 24 h (Figure 3 A). The UV/Vis spectrum of the preheated precursor shows that the absorption band for Au^{III} ions disappeared completely, whereas the plasmon band for Au nanocrystals did not appear (Figure 3 B). Note that no signal attributed to the nanocrystals appeared, even when the preheating lasted for 170 h at 75 °C. In the subsequent reaction upon heating at 125 °C, the color of the solution turned red and then brown as the reaction time increased, reflecting the formation of Au nanocrystals. TEM and

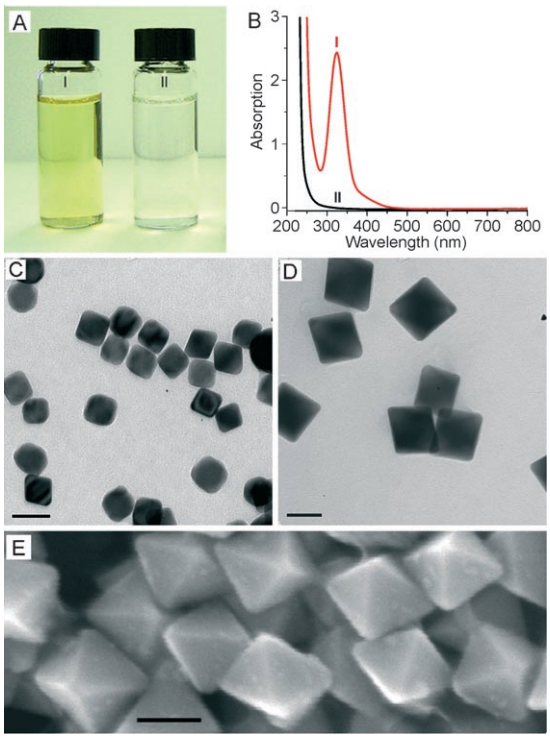

Figure 3. A) Photograph and B) the corresponding UV/Vis spectra of the precursor solution recorded before (I) and after (II) being preheated at 75 °C. Curve (I) in (B) was recorded after the precursor was diluted with ethanol. TEM images of the Au nanocrystals obtained at reaction times of C) 6 h and D) 48 h. E) FESEM image of the sample in (D). All scale bars are 50 nm. (The Au nanocrystals obtained at a reaction time of 24 h are shown in Figures 1 and 2).

FESEM examinations revealed that the octahedral Au nanocrystals obtained at 6, 24, and 48 h had edge lengths of 30, 50, and 60 nm, respectively, with a polydispersity less than 10 % (Figures 1 and 3, and Supporting Information, Figure S1). From these results, we make the following conclusions: 1) Au nano-octahedra were not formed by the preheating process and instead the Au^{III} ions in the precursor were only converted into low-valence Au ions after the preheating.[22] 2) PEG 600 and the surfactant PVP themselves did not contribute to reducing the Au^{III} ions to zero-valent Au^0 atoms at the preheating temperature. 3) Au nano-octahedra were created and grew during the reaction process. 4) The reaction in this modified polyol process is not rapid, probably because of the relatively low reaction temperature; thereby, Au nano-octahedra of various sizes (30–60 nm) were selectively harvested by controlling the reaction time.

As well demonstrated by Wang,[23] the ratio (R) of the growth rate along the ⟨100⟩ to ⟨111⟩ directions determines the geometrical shape of a crystal. The shape of a cubic nanocrystal will evolve from a perfect cube ($R = 0.58$) to a cubo-octahedron ($R = 0.87$), a truncated octahedron ($0.87 < R < 1.73$), and finally to a perfect octahedron ($R = 1.73$) as R increases. This process explains that the octahedral nanocrystals consisting of eight highly stable {111} planes resulted from a much higher growth rate along the ⟨100⟩ direction than along the ⟨111⟩ direction. Generally, the crystal growth rates along different directions are proportional to their surface

energies. For Au with an fcc structure, the surface energy (r) relationships among three low-index crystallographic planes correspond to $r_{\{110\}} > r_{\{100\}} > r_{\{111\}}$.[23] However, the surface energies can be modulated through the selective adsorption of polymers on certain crystal planes,[14,16] which can control the growth rate of the nanocrystals along a certain direction. X-ray photoelectron spectra (XPS) measured for the repeatedly washed sample verifies that PVP molecules were strongly adsorbed on the surface of Au nano-octahedra (Supporting Information, Figure S2). Previous studies[8,14,16,21] revealed that surfactant PVP could act not only as a stabilizer to prevent the aggregation of the products but also as a shape-controller to assist the formation of anisotropic metal nanostructures. In our experiments, when surfactant PVP was absent, the products were dominated by irregularly shaped Au particles (Supporting Information, Figure S3 A), suggesting that the presence of PVP was undoubtedly significant for the synthesis of Au nano-octahedra. On the basis of our results and the previous reports,[5d,11c,16a,21] we believe that PVP preferentially adsorbs on the {111} planes of Au nuclei and consequently the growth rate along the ⟨111⟩ direction is reduced while the growth rate along the ⟨100⟩ direction is enhanced, facilitating the formation of octahedral Au nanocrystals.

Growth rates of nanocrystals in a polyol process are also greatly affected by the reaction temperature which greatly influences the reducing power of polyols and thus the generation rate of source Au atoms.[5d,14] Herein, when the reaction temperature was decreased from 125 to 100 °C, truncated Au nano-octahedra became the major product (Supporting Information, Figure S3 B). In contrast, at higher reaction temperature (> 150 °C), both octahedral Au particles and many quasi-spherical Au nanoparticles were produced (Figure S3 C) and furthermore their size distribution was broad. These results indicate that an appropriate reaction temperature (around 125 °C in this modified polyol process) is essential to obtain Au nano-octahedra in high yield.

Further experiments revealed that the introduction of both the preheating process at a low temperature and the reducing reagent $NaBH_4$ were two key parameters to increase the relative yield of octahedral Au nanocrystals. When the precursor solution was not preheated at 75 °C but instead heated directly to the reaction temperature of 125 °C, the products had various mixed shapes and moreover the particle size increased up to 170–200 nm (Supporting Information, Figure S3 D). In addition, if $NaBH_4$ was not added to the precursor solution, only a few octahedral Au particles mixed with other kinds of Au nanostructures were obtained (Supporting Information, Figure S3 E). However, at higher $NaBH_4$ concentration (> 0.75 mM), the reddish color indicating the formation of Au nanoparticles appeared in less than 30 min of preheating; the final products were dominated by quasi-spherical Au nanoparticles with the sizes of tens nanometers (Supporting Information, Figure S3 F). This result indicates that $NaBH_4$ acts as a strong reducing agent that directly reduces Au^{III} ions in the Au salts to Au^0 atoms. The optimum concentration of $NaBH_4$ for the high-yield synthesis of Au nano-octahedra was 0.15–0.35 mM, which is less than stoichiometric. In this range, the precursor solution became colorless after being preheated at 75 °C. Owing to the less than stoichiometric concentration of $NaBH_4$, only some of the Au^{III} ions were initially reduced to Au^0 atoms, which can then be oxidized by the remained Au^{III} ions (Supporting Information, Figure S4):[24] $NaBH_4$ was used up completely after preheating process.

As described above, no Au^{III} ions and no Au nanocrystals were detected in the UV/Vis spectra of the preheated solution, suggesting that this solution is mostly composed of Au^{I} ions because: 1) Au^{II} ions are very unstable; 2) Au crystals would be formed after a long preheating if the Au was mainly present in the form of atoms. In addition to $NaBH_4$, PEG 600 and PVP also participate in the reduction of Au^{III} ions although their reducing power is much lower than that of $NaBH_4$.[25] Hence, most of the Au^{III} ions were finally converted into Au^{I} ions if a proper (less than stoichiometric) concentration of $NaBH_4$ was used.

After the preheating process, when the reaction temperature was increased above 100 °C, the Au ions were reduced to Au^0 atoms by a so-called polyol process,[5d,20] and thus Au nanocrystals were produced. Our results suggest that almost complete conversion of Au^{III} ions into Au^{I} ions by the preheating process is crucial for the selective formation of octahedral Au nanocrystals. In this case, Au^0 atoms must be generated through the reduction of Au^{I} ions, which is one-step reaction: all the Au^{I} ions can be simply reduced to Au^0 atoms at the reaction temperature and no other Au intermediates can interfere with the nucleation and growth of the crystals. Consequently, only source Au atoms for the nanocrystals are steadily produced, facilitating uniform nuclei formation. It has been observed that the supersaturation gradient needed for anisotropic growth occurs easily at the particle's surface during much slower reactions such as in our case.[26] In our system, with the help of PVP, the growth ratio of many Au nuclei is near $R = 1.73$ at the reaction temperature (125 °C), which leads to the formation of a large number of octahedral Au nanocrystals. Once octahedral Au nanocrystals were created, they served as "seeds" and grew via a seed-mediated approach,[11c,e,27] and this in turn inhibited new nucleation events, particularly at a lower generation rate of source Au atoms. Additionally, a slightly higher supersaturation at the corners than the surfaces enhances the preferential deposition of atoms at the vertexes of the as-formed nanocrystals.[26] Accordingly, the growth rate along the ⟨100⟩ direction is always higher than that along the ⟨111⟩ direction (R should be near 1.73 for no additional shape change of the Au nanocrystals during growing process), and hence the perfect Au nano-octahedra of various sizes were selectively harvested.

The selective synthesis of high-yield Au nano-octahedra with different sizes allowed us to obtain the size-dependent optical properties of Au nano-octahedra (Figure 4). The surface plasmon resonance (SPR) for the 30-nm Au nano-octahedra is located at 545 nm, which is clearly red-shifted compared to spherical Au nanoparticles of the same size (dash line). The red shift is attributed to the anisotropic morphology and the presence of sharp corners. Intense polarizations localize on such structural features typically yielding red-shifts in spectra.[28] Moreover, as the crystal size increased, the SPR peak of the Au nano-octahedra red-

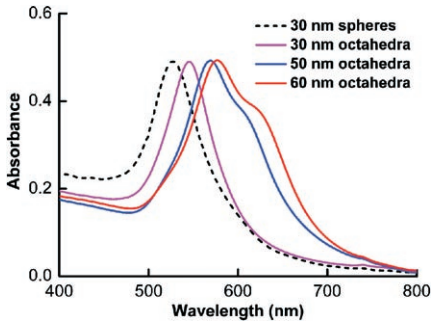

Figure 4. UV/Vis absorption spectra of spherical Au nanoparticles (30 nm) and for nano-octahedra with different edge lengths (30, 50, and 60 nm) dispersed in ethanol.

shifted further than that of nanospheres of the same size. When the edge length of Au nano-octahedra was increased from 30 to 60 nm, the absorption peak red-shifted by approximately 30 nm, while the peak of the spherical nanoparticles red-shifted by less than 15 nm for the same size variation.[29] This result suggests that the optical properties of the Au nano-octahedra are more sensitive to the crystal size than those of the spherical particles. In addition, a new absorption peak appears at a longer wavelength as the size of Au nano-octahedra increases.

The optical properties of octahedral Au nanocrystals in ethanol have been investigated using the DDA.[19] A description of the DDA method and a detailed analysis can be found in the Supporting Information, Figure S5–S9). For labeling purposes, the octahedron was bisected by an imaginary plane into two equivalent square pyramids. The collective oscillation of electrons parallel to the plane was defined as an in-plane mode. The out of plane mode was defined as the collective oscillation of charge perpendicular to this plane. Figure 5 shows the calculated spectra for Au nano-octahedra with 30 and 60 nm edge lengths. The DDA analysis clearly identified that two in-plane dipole modes are excited (Figure S5). One is an edge dipole mode, where the induced polarizations are parallel to the edges of two neighboring corners in the bisecting plane, and the other is a cross dipole mode, where the induced polarizations are oriented diagonally across toward the opposite corners (Supporting Information, Figure S6). The left peak of the spectrum is attributed primarily to the edge dipole mode, while the right peak results primarily from the cross dipole mode; however, the true induced polarization cannot be uncoupled completely owing to the mutual interaction occurring between them. Interestingly, if the nano-octahedra have perfect shape, both in-plane dipole modes are excited simultaneously to varying degrees when the incident field is polarized parallel to the bisecting plane because of strong coupling effects (Supporting Information, Figure S8,S9). However, if the corners of the Au nano-octahedra are slightly truncated, the in-plane modes are excited at the same wavelength producing a single absorption peak (Supporting Information, Figure S6,S7). These results, which agree well with the experimental results, suggest that smaller (30 nm) nano-octahedra have slightly rounded corners but the particles become almost perfect octahedra when they grow to 60 nm. In addition, calculations show that the out-of-plane dipole mode is also excited at a wavelength similar to the in-plane edge dipole excitation, which contributes to the main absorption band (Supporting Information, Figure S5).

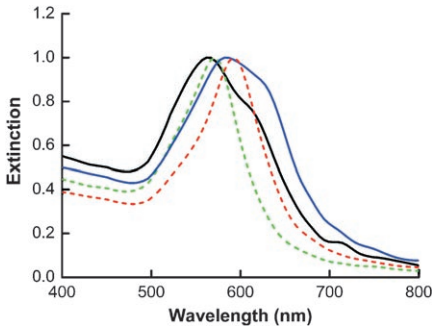

Figure 5. Calculated extinction spectra of Au nanoparticles in ethanol. The black and blue solid traces correspond to nano-octahedra with edge lengths of 30 and 60 nm, respectively. The green and red dashed traces correspond to 30- and 60-nm nano-octahedra, respectively, whose tips are truncated by 3 nm. The peaks are normalized in all traces.

In summary, single-crystalline Au nano-octahedra were successfully synthesized in high yield, with well-defined shape and tunable size (30–60 nm) by a modified polyol process in a PEG 600 solution. This process provides an effective route for the selective synthesis of octahedral Au nanocrystals. Octahedral Au nanocrystals with sharp corners exhibit attractive optical properties, which are sensitive to the crystal size and the truncation of tips. The optical properties of nano-octahedra could have promising applications to surface-enhancement spectroscopic methods, chemical or biological sensing, and the fabrication of nanodevices.

Experimental Section

For a typical synthesis of Au nano-octahedra, PVP (222 mg; K-30; Aldrich; $M_w = 40\,000$) was added to a PEG 600 (20 mL; Aldrich; $M_w = 570$–600) solution in a weighing bottle. The mixture was stirred with a magnetic blender for about 30 min. Then, an $NaBH_4$ solution (0.05 mL, 100 mM; Aldrich) was introduced under stirring. After 1–2 min, an aqueous $AuCl_3$ solution (0.16 mL, 125 mM; Aldrich) was added. These operations were performed at room temperature. The solution appeared yellow owing to the presence of Au^{III} ions. The concentrations of Au^{III} ions, $NaBH_4$, and PVP were about 1 mM, 0.25 mM, and 100 mM, respectively. The vessel containing the solution was transferred to an oil bath and preheated at 75 °C for more than 24 h, then further heated at 125 °C for reaction. In the second heating process, PEG 600, like ethylene glycol, not only serves as a solvent of the precursors but as a reducing agent for the reaction. Finally, the products were collected by centrifugation (15 000 rpm). The products were deposited on the bottom of the tubes, and the solution became colorless, indicating that no Au nanocrystals were in the solution. The precipitate was collected and then washed repeatedly with ethanol or water prior to examination and study. Further experiments, in which the amounts of the reagents were varied, were also conducted to determine the role of the surfactant PVP, the reducing agent $NaBH_4$, as well as preheating.

The products were characterized by FESEM (Hitachi S4300 and FEI XL30), EDS, and TEM (FEI Tecnai F20). The samples for FESEM were prepared by directly depositing the washed products on the stages. The samples for TEM examination were prepared by

putting a droplet of the treated solution on Cu grids coated with thin C film and then evaporating in air at room temperature. XRD spectra were measured on a diffractometer (Philips X'pert PRO with $Cu_{K\alpha}$ radiation) by depositing the sample on glass. XPS measurements for Au nano-octahedra that had been repeatedly washed with water were performed using a VG ESCA2000 X-ray photoelectron spectrometer with an $Mg_{K\alpha}$ excitation source. For optical measurement, the products were first dispersed in ethanol, and then optical absorption spectra were recorded with a spectrophotometer (Cary 5E UV/Vis-NIR) in the wavelength range of 200 to 1100 nm, using an optical quartz cell with a 10-mm path-length.

Received: October 11, 2006
Revised: November 23, 2006
Published online: March 23, 2007

Keywords: crystal growth · gold · nanostructures · polyol synthesis

[1] a) Y. W. Cao, R. C. Jin, C. A. Mirkin, *Science* **2002**, *297*, 1536; b) C. Burda, X. B. Chen, R. Narayanan, M. A. El-Sayed, *Chem. Rev.* **2005**, *105*, 1025; c) N. L. Rosi, C. A. Mirkin, *Chem. Rev.* **2005**, *105*, 1547.

[2] a) K. Kneipp, Y. Wang, H. Kneipp, L. T. Perelman, I. Itzkan, R. R. Dasari, M. S. Feld, *Phys. Rev. Lett.* **1997**, *78*, 1667; b) A. J. Haes, R. P. Van Duyne, *J. Am. Chem. Soc.* **2002**, *124*, 10596; c) B. D. Moore, L. Stevenson, A. Watt, S. Flitsch, N. J. Turner, C. Cassidy, D. Graham, *Nat. Biotechnol.* **2004**, *22*, 1133.

[3] a) I. H. El-Sayed, X. H. Huang, M. A. El-Sayed, *Nano Lett.* **2005**, *5*, 829; b) X. H. Huang, I. H. El-Sayed, W. Qian, M. A. El-Sayed, *J. Am. Chem. Soc.* **2006**, *128*, 2115.

[4] a) R. C. Jin, Y. W. Cao, C. A. Mirkin, K. L. Kelly, G. C. Schatz, J. G. Zheng, *Science* **2001**, *294*, 1901; b) R. C. Jin, Y. C. Cao, E. Hao, G. S. Métraux, G. C. Schatz, C. A. Mirkin, *Nature* **2003**, *425*, 487.

[5] a) J. U. Kim, S. H. Cha, K. Shin, J. Y. Jho, J. C. Lee, *Adv. Mater.* **2004**, *16*, 459; b) X. P. Sun, S. J. Dong, E. K. Wang, *Langmuir* **2005**, *21*, 4710; c) Z. Li, Z. Liu, J. Zhang, B. Han, J. Du, Y. Gao, T. Jiang, *J. Phys. Chem. B* **2005**, *109*, 14445; d) C. C. Li, W. P. Cai, B. Q. Cao, F. Q. Sun, Y. Li, C. X. Kan, L. D. Zhang, *Adv. Funct. Mater.* **2006**, *16*, 83.

[6] a) N. Malikova, I. Pastoriza-Santos, M. Schierhorn, N. A. Kotov, L. M. Liz-Marzán, *Langmuir* **2002**, *18*, 3694; b) T. K. Sau, C. J. Murphy, *J. Am. Chem. Soc.* **2004**, *126*, 8648; c) J. E. Millstone, S. Park, K. L. Shuford, L. D. Qin, G. C. Schatz, C. A. Mirkin *J. Am. Chem. Soc.* **2005**, *127*, 5312.

[7] a) S. S. Shankar, A. Rai, B. Ankamwar, A. Singh, A. Ahmad, M. Sastry, *Nat. Mater.* **2004**, *3*, 482; b) S. S. Shankar, A. Rai, A. Ahmad, M. Sastry, *Chem. Mater.* **2005**, *17*, 566.

[8] a) Y. G. Sun, B. Gates, B. Mayers, Y. N. Xia, *Nano Lett.* **2002**, *2*, 165; b) J. H. Song, F. Kim, D. Kim, P. D. Yang, *Chem. Eur. J.* **2005**, *11*, 910.

[9] a) F. Kim, J. H. Song, P. D. Yang, *J. Am. Chem. Soc.* **2002**, *124*, 14316; b) B. D. Busbee, S. O. Obare, C. J. Murphy, *Adv. Mater.* **2003**, *15*, 414; c) B. Nikoobakht, M. A. El-Sayed, *Chem. Mater.* **2003**, *15*, 1957; d) J. Pérez-Juste, I. Pastoriza-Santos, L. M. Liz-Marzán, P. Mulvaney, *Coord. Chem. Rev.* **2005**, *249*, 1870.

[10] a) X. P. Sun, S. J. Dong, E. K. Wang, *Angew. Chem.* **2004**, *116*, 6520; *Angew. Chem. Int. Ed.* **2004**, *43*, 6360; b) C. S. Ah, Y. J. Yun, H. J. Park, W. J. Kim, D. H. Ha, W. S. Yun, *Chem. Mater.* **2005**, *17*, 5558; c) C. X. Kan, G. H. Wang, X. G. Zhu, C. C. Li, B. Q. Cao, *Appl. Phys. Lett.* **2006**, *88*, 071904; d) C. X. Kan, X. G. Zhu, G. H. Wang, *J. Phys. Chem. B* **2006**, *110*, 4651.

[11] a) I. Pastoriza-Santos, L. M. Liz-Marzán, *Nano Lett.* **2002**, *2*, 903; b) G. S. Métraux, C. A. Mirkin, *Adv. Mater.* **2005**, *17*, 412; c) C. C. Li, W. P. Cai, Y. Li, J. L. Hu, P. S. Liu, *J. Phys. Chem. B* **2006**, *110*, 1546; d) V. Bastys, I. Pastoriza-Santos, B. Rodríguez-González, R. Vaisnoras, L. M. Liz-Marzán, *Adv. Funct. Mater.* **2006**, *16*, 766; e) J. E. Millstone, G. S. Mtraux, C. A. Mirkin, *Adv. Funct. Mater.* **2006**, *16*, 1209.

[12] a) Y. G. Sun, B. Mayers, Y. N. Xia, *Nano Lett.* **2003**, *3*, 675; b) J. L. Zhang, J. M. Du, B. X. Han, Z. M. Liu, T. Jiang, Z. F. Zhang, *Angew. Chem.* **2006**, *118*, 1134; *Angew. Chem. Int. Ed.* **2006**, *45*, 1116.

[13] a) S. H. Chen, Z. L. Wang, J. Ballato, S. H. Foulger, D. L. Carroll, *J. Am. Chem. Soc.* **2003**, *125*, 16186; b) E. Hao, R. C. Bailey, G. C. Schatz, J. T. Hupp, S. Y. Li, *Nano Lett.* **2004**, *4*, 327.

[14] a) Y. G. Sun, Y. N. Xia, *Science* **2002**, *298*, 2176; b) B. J. Wiley, Y. G. Sun, B. Mayers, Y. N. Xia, *Chem. Eur. J.* **2005**, *11*, 454; c) S. H. Im, Y. T. Lee, B. Wiley, Y. N. Xia, *Angew. Chem.* **2005**, *117*, 2192; *Angew. Chem. Int. Ed.* **2005**, *44*, 2154.

[15] a) R. C. Jin, S. Egusa, N. F. Scherer, *J. Am. Chem. Soc.* **2004**, *126*, 9900; b) D. B. Yu, V. W.-W. Yam, *J. Am. Chem. Soc.* **2004**, *126*, 13200; c) Y. Chen, X. Gu, C.-G. Nie, Z.-Y. Jiang, Z.-X. Xie, C.-J. Lin, *Chem. Commun.* **2005**, 4181.

[16] a) F. Kim, S. Connor, H. Song, T. Kuykendall, P. D. Yang, *Angew. Chem.* **2004**, *116*, 3759; *Angew. Chem. Int. Ed.* **2004**, *43*, 3673; b) A. Tao, P. Sinsermsuksakul, P. D. Yang, *Angew. Chem.* **2006**, *118*, 4713; *Angew. Chem. Int. Ed.* **2006**, *45*, 4597; c) D. Seo, J. C. Park, H. Song, *J. Am. Chem. Soc.* **2006**, *128*, 14863.

[17] a) A. Sánchez-Iglesias, I. Pastoriza-Santos, J. Pérez-Juste, B. Roríguez-González, F. J. G. Abajo, L. M. Liz-Marzán, *Adv. Mater.* **2006**, *18*, 2529; b) J. Zhang, Y. Gao, R. A. Alvarez-Puebla, J. M. Buriak, H. Fenniri, *Adv. Mater.* **2006**, *18*, 3233; c) X. Liu, N. Wu, B. H. Wunsch, R. J. Barsotti Jr. , F. Stellacci, *Small* **2006**, *2*, 1046.

[18] B. J. Wiley, Y. J. Xiong, Z. Y. Li, Y. D. Yin, Y. N. Xia, *Nano Lett.* **2006**, *6*, 765.

[19] a) B. T. Draine, *Astrophys. J.* **1988**, *333*, 848; b) B. T. Draine, P. J. Flatau, *J. Opt. Soc. Am. A* **1994**, *11*, 1491.

[20] F. Fievet, J. P. Lagier, M. Figlarz, *MRS Bull.* **1989**, *14*, 29.

[21] a) M. Tsuji, M. Hashimoto, Y. Nishizawa, M. Kubobawa, T. Tsuji, *Chem. Eur. J.* **2005**, *11*, 440; b) M. Tsuji, N. Miyamae, S. Lim, K. Kimura, X. Zhang, S. Hikino, M. Nishio, *Cryst. Growth Des.* **2006**, *6*, 1801.

[22] N. R. Jana, L. Gearheart, C. J. Murphy, *Langmuir* **2001**, *17*, 6782.

[23] Z. L. Wang, *J. Phys. Chem. B* **2000**, *104*, 1153.

[24] J. Rodríguez-Fernández, J. Pérez-Juste, P. Mulvaney, L. M. Liz-Marzán, *J. Phys. Chem. B* **2005**, *109*, 14257.

[25] a) I. Pastoriza-Santos, L. M. Liz-Marzán, *Langmuir* **2002**, *18*, 2888; b) C. E. Hoppe, M. Lazzari, I. Pardiñas-Blanco, M. A. López-Quintela, *Langmuir* **2006**, *22*, 7027; c) I. Washio, Y. J. Xiong, Y. D. Yin, Y. N. Xia, *Adv. Mater.* **2006**, *18*, 1745.

[26] a) A. Nielsen, *Kinetics of Precipitation*, Pergamon, New York, **1964**; b) A. Chernov, *Sov. Phys.-Crystallogr.* **1972**, *16*, 734; c) T. Herricks, J. Y. Chen, Y. N. Xia, *Nano Lett.* **2004**, *4*, 2367.

[27] a) N. R. Jana, L. Gearheart, C. J. Murphy, *Chem. Mater.* **2001**, *13*, 2313; b) J. Rodríguez-Fernández, J. Pérez-Juste, F. J. G. Abajo, L. M. Liz-Marzán, *Langmuir* **2006**, *22*, 7007.

[28] a) K. L. Kelly, E. Coronado, L. L. Zhao, G. C. Schatz, *J. Phys. Chem. B* **2003**, *107*, 668; b) J. Aizpurua, G. W. Bryant, L. J. Richter, F. J. García de Abajo, B. K. Kelley, T. Mallouk, *Phys. Rev. B* **2005**, *71*, 235420.

[29] S. Link, M. A. El-Sayed, *J. Phys. Chem. B* **1999**, *103*, 8410.

